Influence of sodium silicate powder silica modulus for mechanical and chemical properties of dry-mix alkali-activated slag mortar

Tero Luukkonen[1], Harisankar Sreenivasan[1], Zahra Abdollahnejad[1], Juho Yliniemi[1], Anu Kantola[2], Ville-Veikko Telkki[2], Paivo Kinnunen[1], Mirja Illikainen[1]

[1]Fibre and Particle Engineering Research Unit, P.O. Box 4300, FI-90014, University of Oulu, Finland

[2] NMR Research Unit, Faculty of Science, P.O. Box 4300, 90014 University of Oulu, Finland

Corresponding author: Tero Luukkonen, tero.luukkonen@oulu.fi

Declarations of interest: none

Abstract

Sodium silicate powders with different SiO_2/Na_2O (silica modulus) were characterized by solubility rate, pH, and chemical structure (by ^{29}Si MAS-NMR) and compared in the preparation of one-part (or dry-mix) alkali-activated blast furnace slag mortar. The low SiO_2/Na_2O indicated the beneficial presence of less-polymerized silica (Q^1 and Q^2) and thus faster dissolution. Consequently, using silicates with SiO_2/Na_2O of 0.9, 2.1, and 3.4 resulted 28 d compressive strengths of 103, 80, and 2 MPa, respectively, with increasing setting time and decreasing heat release in isothermal calorimetry. Adjustment of activator SiO_2/Na_2O (from 2.1 or 3.4 to 0.9) by adding NaOH powder resulted increased or decreased mechanical properties of mortar, respectively. These properties were not, however, similar to obtained with sodium silicate having SiO_2/Na_2O of 0.9 originally. Depending on the case, the added NaOH can be consumed for dissolving sodium silicate activator, slag, or the forming (C,N)-(A)-S-H gel.

Keywords: Blast furnace slag; Dry-mix mortar; Geopolymer; One-part alkali-activated material, Sodium silicate; Silica modulus

1. Introduction

Alkali-activated materials (AAMs), including geopolymers, have gained acceptance as a potentially environmentally-friendly alternative to Portland cement [1]. Examples of recent construction projects that have utilized AAMs include the University of Queensland's Global Change Institute (2013, Australia); the Toowoomba Wellcamp Airport (2014, Australia); and Transnet's City Deep Container Terminal (2015, South Africa). Alkali-activated blast furnace slag (BFS), alone or in combination with other precursors, is one of the most actively studied AAM binders. Conventional AAMs employ high-viscosity and frequently corrosive alkali-activator solutions, which typically consist of concentrated aqueous alkali hydroxide and/or silicate [1]. However, to avoid the impracticalities and occupational hazards of handling these solutions, various one-

part (i.e., dry-mix or “just add water”) AAMs have been increasingly studied [2]. One-part AAMs use a solid powder alkali-activator, and the reactions are initiated by adding water. One of the earliest examples of one-part AAMs was published in 1940 by Purdon [3]: BFS activated by solid sodium hydroxide. However, as one potential drawback, the use of solid-state activators in comparison to similar solutions can result lower strength in some cases [4]. Nevertheless, one-part AAMs containing BFS and class F fly ash have been commercialized recently [5-7].

The selection of the solid activator is essential for the successful development of high-strength and durable one-part AAM binders. The solid activators employed with BFS have included alkali silicates, hydroxides, carbonates, calcium oxide, and calcium hydroxide either alone or in combination [2]. Also environmentally friendly alternative activators based various industrial by-products such as rice husk ash [8], maize cob ash [9,10], or waste glass [11] could be used. These industrial by-products have sufficiently high alkali and/or silica content together with high pH, which enables their use as solid activators. In general, sodium silicates result the most promising properties [12]. Although synthetic sodium silicates are relatively expensive and have a large environmental footprint in comparison to other activators [13], they could still be used in applications that require especially high strength. Furthermore, high-strength concrete requires thinner structures to have performance similar to regular concrete, which reduces costs, structural self-weight, and the duration of construction.

However, not all sodium silicate grades result in good performance. The main variables to consider are the silica modulus (i.e., the ratio of SiO_2/Na_2O, R_M) and the amount of chemically-bound water. Ma et al. [14] compared solid sodium silicate activators for BFS with different amounts of water (anhydrous, pentahydrate, or nonahydrate), but with similar silica moduli (R_M = 1.06–1.07). They reported that anhydrous sodium silicate had the highest compressive strength (≈ 80 MPa at 60 d) followed by nonahydrate (≈ 70 MPa at 60 d) and pentahydrate (≈ 60 MPa at 60 d) [14]. In an earlier study, Nematollahi et al. [15] obtained similar results; anhydrous sodium silicate (R_M = 0.93) performed better than pentahydrate or GD grade sodium silicate (R_M = 1.00 and 2.06, respectively) as activators for BFS and class F fly ash. Highly hydrated solid sodium silicates can contain up to 60 wt% of chemically bound water; thus, the amount of the activator in the AAM binder must be increased accordingly [14].

The aforementioned studies have focused on the effect of chemically-bound water in solid sodium silicates but the effect of the silica modulus is documented less systematically. Wang and Scrivener [4] recommended using anhydrous solid sodium silicate with $R_M < 1.2$. Collins and Sanjayan [16] mixed two powdered sodium silicates (R_M = 1.0 and 2.1) to obtain solid activators with silica moduli between 1.0–1.8. Their results indicated that early strength of pastes prepared of BFS and sodium silicate mixture decreased as the silica modulus increased [16]. Similar results were reported by Ravikumar and Neithalath [17], who prepared mixtures of solid sodium silicate (R_M = 1.95) with solid NaOH to obtain silica moduli between 0.62–1.55 and used this as an alkali activator for BFS. The prepared mortars exhibited decreased early strength (at 3 and 7 d) but increased strength at 28 d as the silica modulus increased in this range [17]. Summary of these and other studies involving BFS as the precursor and sodium silicate powder as the activator are shown in Table 1 (a more comprehensive review about one-part AAMs is available in [2]). As can be seen, the silica modulus of sodium silicates has varied within 0.9–1.1. However, there are commercially available solid sodium silicates with higher silica moduli but their suitability for one-part alkali-activated systems has not been documented.

Table 1. Summary of earlier studies involving BFS as precursor and solid sodium silicate as activator. Curing was conducted at room temperature and relative humidity of 70–100% in every study.

Solid activators	Properties of sodium silicate		Mix design			Compressive strength [MPa]		Ref.
	R_M	Water [%]	Activator [a]	Fine aggregate [b]	Water [c]	7 d	28 d	
Sodium silicate	< 1.2	0	n.r.	n.r.	n.r.	n.r.	10–80	[4]
Sodium silicate	1.1	< 1.0	0.10	0	0.35	≈ 62	≈ 75	[14]
Sodium silicate	1.0	42.5	0.19	0	0.35	≈ 45	≈ 53	[14]
Sodium silicate	1.0	57.1	0.26	0	0.35	≈ 55	≈ 72	[14]
Sodium silicate	0.9	2.5	0.10	2.0	0.35	91.4	107.4	[18]
Sodium silicate, NaOH	0.62–1.55 [d]	n.r.	n.r.	n.r.	0.40	5–11	15–30	[17]
Sodium silicate	0.9	4.8	0.38	3.0	0.5	47.1	51.3	[19]
Sodium silicate	0.9	4.8	n.r.	3.0	0.3	64.5	71.6	[20]
Sodium silicate	0.9	4.8	0.22	3.0	0.5	49.3	53.8	[21]
Sodium silicate, lime	1.0	43	n.r.	2.3 [e]	0.5	≈ 37	≈ 45	[22]
Sodium silicate, lime	1.0	n.r.	n.r.	3.0	0.5	≈ 36	≈ 42	[16]
Sodium silicate, lime	n.r.	n.r.	n.r.	2.3 [e]	0.5	≈ 48	≈ 58	[23]
Sodium silicate, lime	n.r.	n.r.	n.r.	2.3 [e]	0.5	≈ 35–42 [f]	≈ 40	[24]
Sodium silicate, lime	n.r.	n.r.	n.r.	2.3 [e]	0.5	≈ 43	≈ 51	[25]

[a] weight ratio sodium silicate / BFS; [b] = weight ratio aggregate / binder (binder = BFS + activator); [c] = weight ratio water/binder; [d] = silica modulus adjusted with NaOH; [e] = also coarse aggregate (< 14 mm) was used, total aggregate to binder = 5.4; [f] = depending on the aggregate type

In the present study, the research questions were 1) how do the solid sodium silicates with different R_M differ in terms of their chemical structure and properties; 2) how does the R_M of solid sodium silicate affect the chemical and mechanical properties of one-part alkali-activated BFS mortar; and 3) how does solid NaOH mixed with solid sodium silicate affect the aforementioned properties. The hypothesis was, based on literature (see Table 1), that a low R_M (≈ 1) of solid sodium silicate should result high strength. However, studies with solid sodium silicates with R_M larger than approximately 1.6 (Table 1) have been sparingly reported and thus represent a knowledge gap. Therefore, in this study, commercial sodium silicates (R_M = 0.9, 2.1, 3.4, and 3.5) were tested to understand the relationship between the solid sodium silicate chemical properties, structure, and the resulting one-part alkali-activated BFS mortar properties. Furthermore, it was tested whether it is possible to modify the R_M of solid sodium silicates (from 2.1 or 3.4 to 0.9) by adding solid sodium hydroxide (NaOH) and this was compared with sodium silicate originally having R_M = 0.9. The cost and CO_2-equivalent emissions of silicate grades vary [14]; thus, it is important to understand their suitability as solid activators in one-part AAMs to balance the performance and environmental impacts.

2. Materials and methods

2.1. Materials

The ground-granulated BFS (Finnsementti, Finland) used in this study had the d_{10}, d_{50}, and d_{90} values of 0.9, 10.8, and 51.7 µm, respectively (see supplementary material for the full particle size distribution). Bulk and true densities of BFS were 1.20 and 2.93 g/cm^3, respectively, as reported by the supplier. Loss on ignition

(LOI) of BFS was 0.46% (at 950°C). The chemical composition of BFS is shown in Table 2. This study used the following solid sodium silicate activators: anhydrous sodium metasilicate (abbreviated as Rm0.9), Sikalon A (Rm2.1), Sikalon N 601 (Rm3.4), and sodium trisilicate (Rm3.5). Their properties and manufacturer information are shown in Table 3. NaOH powder (≥ 97% purity; Honeywell, Germany) was used to adjust the silica moduli of Rm2.1 and Rm3.4 in the selected mixes. Standard sand (Normensand, Germany) was used for the preparation of mortars. The sand had particle size ranging between 0.08–2 mm.

Table 2. The chemical composition of BFS as determined using X-ray fluorescence.

Oxide [wt%]	Blast furnace slag (BFS)
Na_2O	0.51
MgO	10.24
Al_2O_3	9.58
SiO_2	32.33
P_2O_5	0.01
SO_3	4.00
K_2O	0.53
CaO	38.51
Fe_2O_3	1.23

Table 3. Properties of the sodium silicates as reported by the manufacturers.

Commercial name	Anhydrous sodium metasilicate	Sikalon A	Sikalon N 601	Sodium trisilicate
Manufacturer	Alfa Aesar, Germany	Wöllner GmbH, Germany	Wöllner GmbH, Germany	VWR Chemicals
Chemical formula	$SiO_2 \cdot Na_2O$	$2SiO_2 \cdot Na_2O \cdot nH_2O$	$3SiO_2 \cdot Na_2O \cdot nH_2O$	$3SiO_2 \cdot Na_2O \cdot nH_2O$
Abbreviation used in the text	Rm0.9	Rm2.1	Rm3.4	Rm3.5
Na_2O [wt%]	50.8	27.5	19.0	19.2
SiO_2 [wt%]	46.7	56.0	61.0	63.9
Water [wt%]	2.5	16.5	20	16.9
R_M, molar SiO_2/Na_2O	0.9	2.1	3.4	3.5

2.2. Preparation of the alkali-activated BFS mortar

The mix design was based on an earlier study [18]. The binder consisted of 90 wt% BFS and 10 wt% of solid sodium silicate. The mix design was (as a weight ratio): sand/binder/water = 5.7/2.9/1.0. The standard mortar mix design (sand/binder/water = 6:2:1) was not used as it resulted too high water content and consequently bleeding of mortar (more information is provided in the supplementary material). It should be noted that the employed water content does not include chemically-bound water from sodium silicates, which contributed extra 1–5% water. However, decreasing water amount was not possible especially with Rm2.1 since the mortar became too stiff and unworkable. Therefore, the added water amount was kept constant for all mixes. The mortar was prepared by mixing dry solids for 3 min, adding water, and mixing for another 3 min. The mixture was cast in a 40 × 40 × 160 mm prismatic mold coated with mold oil and compacted using a jolting table (2 × 60 shocks, 1 shock/s). The mold was placed in a curing chamber (22°C and 100% relative humidity) for approximately 24 h. Then, the specimens were demolded and returned to the curing chamber until tested.

With Rm2.1 and Rm3.4, NaOH powder was added to decrease their silica moduli from 2.1 and 3.4, respectively, to 0.9. These mixes are abbreviated as Rm2.1 + NaOH and Rm3.4 + NaOH. The purpose of the addition was to compare Rm0.9 with the modified silicates.

2.3. Characterization methods

The chemical composition of BFS was determined using a 4 kV wavelength dispersive X-ray fluorescence (XRF) spectrometer (PANalytical AxiosmAX). XRF analyses were performed from the fused samples: 1.5 g of the sample was melted at 1150°C with 7.5 g of X-ray Flux Type 66:34 (66 wt% $Li_2B_4O_7$ and 34 wt% $LiBO_2$) to obtain melt-fused tablets. The XRF data was interpreted using the Omnian software. Particle size distribution of BFS was determined by Beckman Coulter LS 13320 laser diffraction particle size analyzer using an oven-dried (105° for 24 h) sample. Loss on ignition (LOI) of BFS was determined by determining a mass decrease of a constant weight sample (dried at 105 °C for 24 h) when heated to 950°C.

To understand the chemical structure of the selected solid activators, the ^{29}Si nuclear magnetic resonance (NMR) spectra of solid sodium silicates were obtained with a Bruker Avance-III 300 spectrometer operating at 59.65 MHz for ^{29}Si. For the magic angle spinning (MAS) experiments, the samples were packed into 7 mm zirconia rotors, then a rotation frequency of 7 kHz was applied and 8192 scans were accumulated with a repetition rate of 3 s. The chemical shifts were referenced to tetramethylsilane (TMS) set to 0 ppm. The ^{29}Si MAS-NMR spectra were deconvoluted into Gaussian components representing Q^n species (in the Q^n notation, n represents the number of bridging oxygen atoms surrounding the silicon atom). Two methods were used to ensure the accuracy of the deconvolution. First, reasonable values for the chemical shift and the full width at half maximum for each Q^n species were selected according to what was reported in earlier literature [26-29]. Second, the experimental ratios (obtained through spectral deconvolution) and theoretical ratios (based on chemical composition) of the non-bridging oxygens to SI were compared.

In order to further compare the properties of selected solid activators, solubility and pH of the solid activators were evaluated by placing 1 g of solid sodium silicate in 1 L of deionized water. Samples (10 mL) for Si determination were taken and pH was measured at 1, 30, 60, and 120 min. The samples were centrifuged (6000 rpm for 5 min) to separate solids, and the supernatant was decanted; then, an inductively coupled optical emission spectrometer (Thermo Electron IRIS Intrepid II XDL Duo) was used to quantify Si concentration. Deionized water without the addition of silicate was measured as a blank sample. The Si analysis was conducted following the standard EN ISO 11885 [30].

The heat release during curing and hardening to assess ongoing chemical processes was determined with isothermal calorimetry. The experiments were conducted with a TAM Air isothermal calorimeter and 20 mL glass admix ampoules equipped with a stirrer (TA Instruments) at a temperature of 25 ± 0.01°C. Solid sodium silicate, BFS, and sand (0.338, 3.038, and 6.750 g, respectively) were loaded into the ampoule while water (1.2 g) was loaded into two, 1 mL syringes. An ampoule filled 1.2 g of water as used as a reference. Samples and reference were first given 4 h to equilibrate inside the calorimeter chamber; then water was added and they were mixed for 3 min using the admix ampoule stirrer. The heat release rate values were normalized by the mass of solid sodium silicate and BFS.

To gain information about the reaction products in studied one-part systems, X-ray diffraction (XRD) analysis was performed using a Rigaku Smartlab diffractometer (9 kW Cu X-ray source) in the range of 10–60 °2θ using 6 °2θ/min scan speed. XRD analysis were conducted on paste samples (i.e., without sand to exclude the quartz signal) and at the age of 28 d. Before analysis, samples were pulverized using a Retsch RS200 mill. Quantification of crystalline phases was performed using the Rietveld refinement method with 10 wt% of rutile (≥ 99.9% purity; Aldrich) as internal standard.

Initial and final setting times were determined at 22°C with a Vicat apparatus (Vicatronic Matest) on paste samples following the standard EN 196-3 [31]. Compressive strength was determined from mortar prisms using a Zwick/Roell Z100 testing machine (maximum force 100 kN) or a Toni Technik 3000 kN testing machine (when > 100 kN force was required). The compressive strength was evaluated from half-beams using a 2.4 kN/s loading rate, according to the standard EN 196-1 [32].

3. Results and discussion

3.1 ^{29}Si NMR characterization of the sodium silicates

^{29}Si MAS-NMR measurements were used to determine the chemical environments of the Si atoms in the solid sodium silicates, as described by the Q^n notation, where: n (0–4) is the number of shared corners of a SiO_4 tetrahedron (i.e., the number of bridging and non-bridging oxygens are n and 4-n, respectively). This information is essential in understanding the behavior of solid sodium silicates as activators in dry-mix alkali-activated BFS mortars.

The increase in the silica modulus of solid sodium silicate is associated with the presence of more connected Si centers: the proportion of Q^1 and Q^2 decreases, while Q^3 and Q^4 increase (Fig. 1). This observed trend is similar to aqueous alkali silicate solutions (used with conventional two-part alkali-activated materials): the larger silica modulus indicates the presence of less depolymerized silica species [33,34]. It is noticeable that there is no Q^0 present (i.e., silica monomers for which the chemical shift would occur in -60 to -80 ppm [35]). As a comparison, the relative quantities of Si centers present in a concentrated sodium silicate solution ([Si] = 7 mol/L, Si/Na = 1.71, and pH = 11.56) followed the order Q^3 (52%) > Q^2 (26%) > Q^4 (15%) > Q^1 (6%) > Q^0 (< 1%) in one study and the predominant species was a $Si_7O_{18}H_4Na_4$ neutral complex [36]. Based on the results of current study, it appears that the proportion of Q^1 and Q^2 are the important Si environments for the reactivity and subsequent strength development in one-part alkali-activated BFS: when comparing Rm2.1 and Rm3.4 (Fig. 1), the proportion of Q^1 + Q^2 decreases from 35.5% to 22.9% with deleterious effects on mechanical strength (see Fig. 7). Other implications of the ^{29}Si MAS-NMR results on the resulting mortar properties are discussed in detail in the following sections.

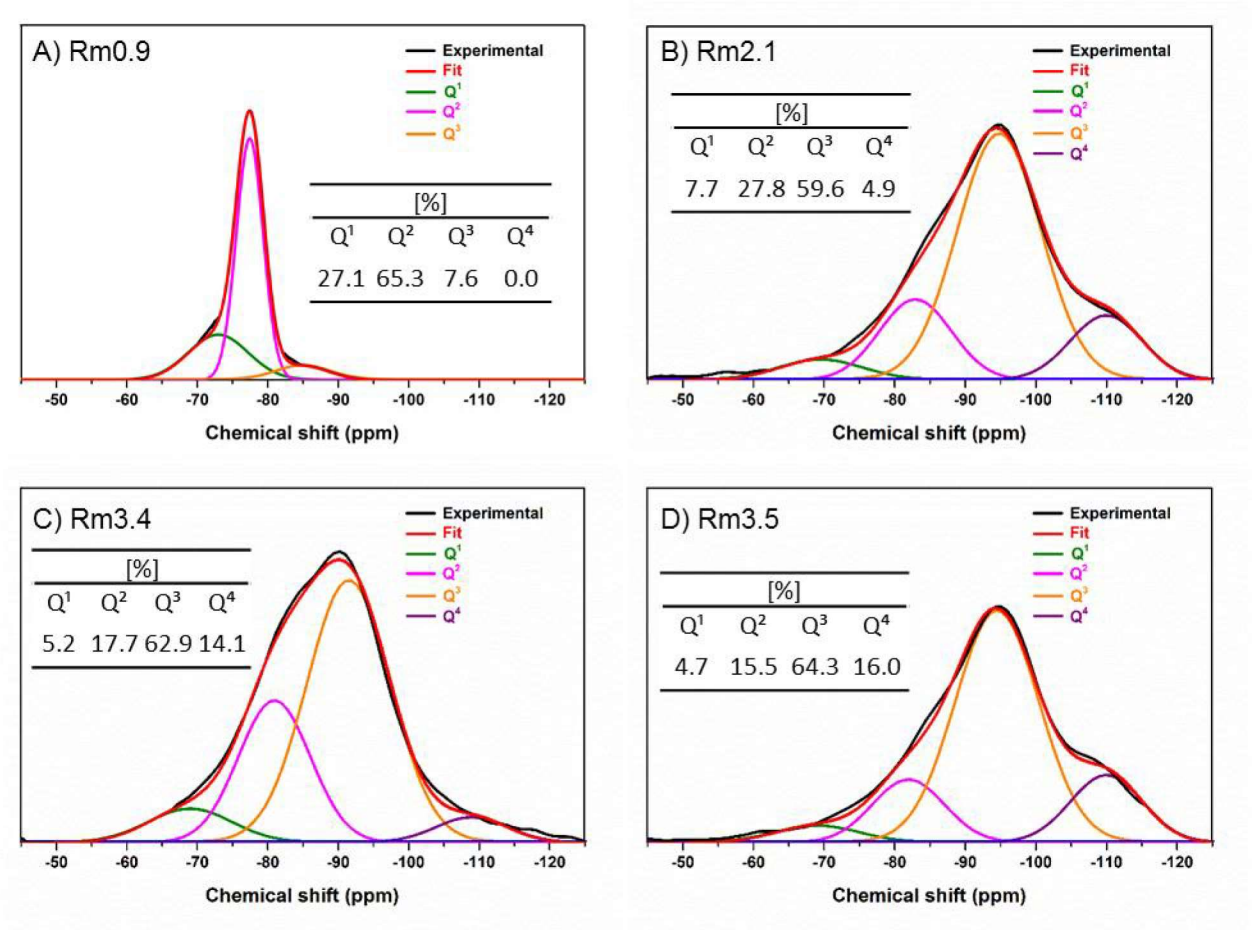

Fig. 1. Deconvoluted ^{29}Si MAS-NMR spectra of the studied solid sodium silicates and distribution of the Si centers into Q^1–Q^4.

3.2 Sodium silicate solubility and pH

The pH of solid sodium silicate is an important parameter as it affects the initial dissolution of BFS [37]. In the following experiments, pH of solid sodium silicate was monitored in a relatively dilute aqueous solution to gain information about the behavior of different sodium silicates in comparison to each other. As solid silicates are mixed with water, pH increases up to a specific value, and then it begins to decrease (Fig. 2). The observed maximum pH decreases linearly as the silica modulus increases (see supplementary data). This is expected because the silica modulus also describes alkalinity: solid alkali silicates with silica moduli of 2.1 and 3.4 are referred to as alkaline and neutral, respectively [38]. In alkali silicate solutions, the silica modulus > 1.45 is considered to be user-friendly because it is merely irritant, not corrosive, due to its lower pH [39]. The decrease of pH shown in Fig. 2 is due to the depolymerization of the Si species, which is known to be facilitated by hydroxyl ions [40]. The hydroxyl ion acts catalytically (i.e., it is regenerated after reaction) when the pH is significantly lower than 11 [40], which was not the case in the experiments presented in Fig. 2. Therefore, hydroxyl ions are consumed for depolymerization, which is the reason for the decrease in pH. With Rm0.9, the pH of the solution remains approximately constant because the amount of highly connected Si centers,Q^3 and Q^4, is low. When NaOH is added to the solutions, the pH is 0.25–0.50 units higher, but the trend is similar to that of the solutions without NaOH: the pH increases to a certain maximum and then it decreases (Fig. 2C, D). Finally, it should be noted that the concentration of sodium silicate in the actual mortar

systems is approximately 285.7 times higher compared to this pH experiment. Therefore, the pH in the actual system can be estimated by assuming that the concentration of OH^- is also approximately 285.7 times higher (i.e., pH is 1.20–1.23 times higher). An example how this was calculated is provided in supplementary materials. Consequently, the calculated initial pH in the real mortar systems would be 14.2 (Rm0.9), 13.8 (Rm2.1), 13.5 (Rm3.4), 13.4 (Rm3.5), 14.2 (Rm2.1 + NaOH), and 14.4 (Rm3.4 + NaOH). The pH observed with the low silica modulus sodium silicates (Rm0.9 and Rm2.1) is approximately 0.5 units higher than with the high silica modulus sodium silicates (Rm3.4 and Rm3.5). Moreover, it appears that pH of Rm0.9 and Rm2.1 + NaOH or Rm3.4 + NaOH is approximately similar but these activators result completely different properties in terms of strength and setting time of mortars. Therefore, pH of solid activator alone is not able to fully account differences in fresh and hardened properties. Another difference between the experiments in deionized water and in the real mortar system is that hydroxyl ions can be consumed also for other reactions than depolymerizing sodium silicates in the latter (this is further discussed in the next sections) and precipitation begins to occur in concentrated aqueous solutions.

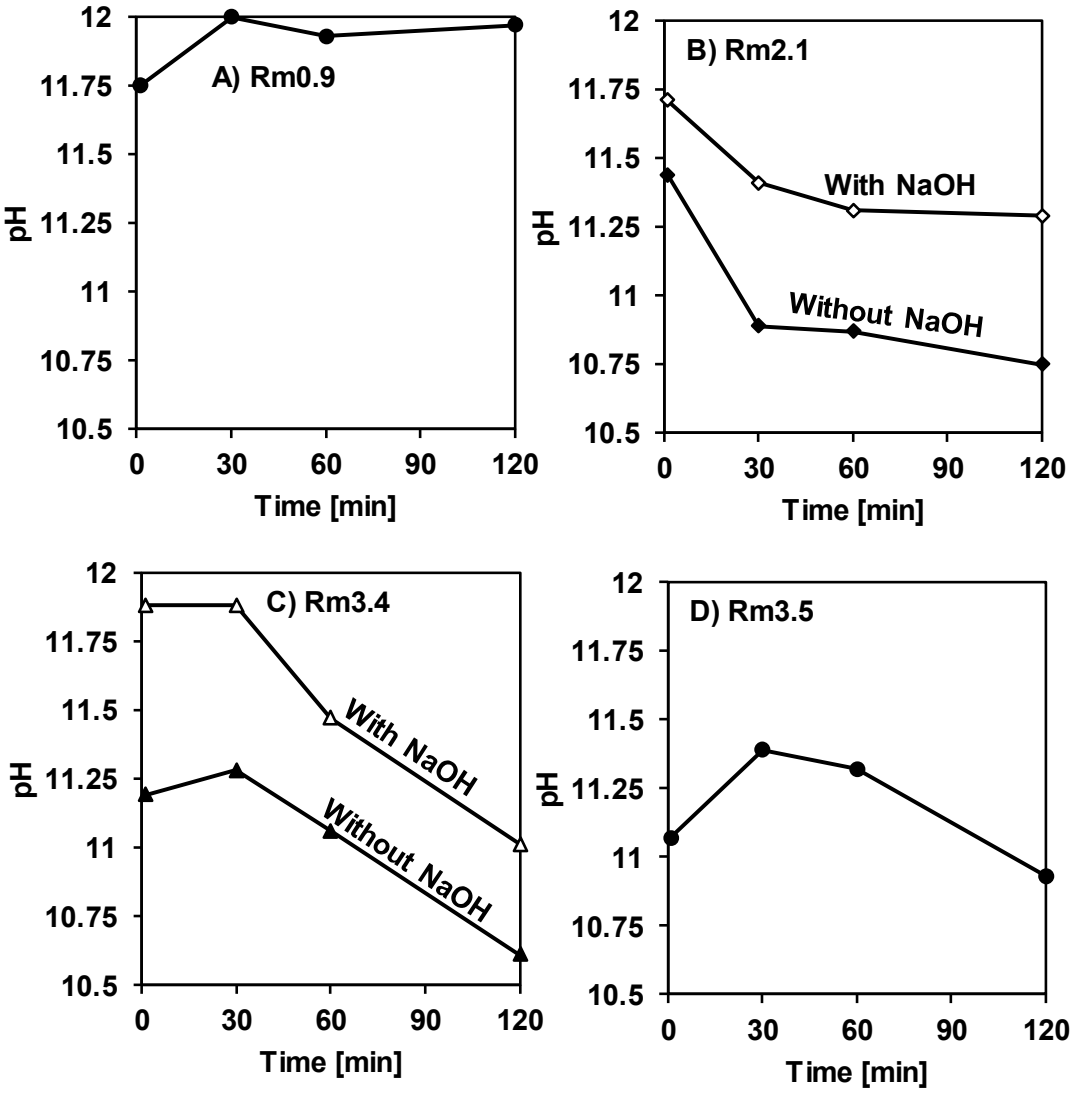

Fig. 2. pH of the sodium silicates (solid/liquid weight ratio = 0.001) in deionized water. The pH in the actual mortar systems can be calcuted as 1.20–1.23 times higher.

The dissolution rate of the solid sodium silicates increases as the silica modulus decreases (Fig. 3) because a low silica modulus indicates higher alkalinity and hydroxyl ions are required for dissolution (or depolymerization) of solid silicates. Solid alkali silicates with $SiO_2/Na_2O > 3.1$ are known to dissolve slowly in water at room temperature [38], as also indicated in the present study (Fig. 3B, 3C). The addition of NaOH significantly increases the dissolution rate in the case of Rm3.4, which has a high proportion of Q^3 Si environments and some Q^4 Si environments. However, Rm2.1 dissolves rapidly already without added NaOH due to a higher proportion of less-connected Si centers (Fig. 1). Therefore, the addition of NaOH only marginally affects the dissolution rate. Finally, the water-to-binder weight ratio is clearly lower in the studied mortar (0.35) than the water-to-solid weight ratio in the solubility experiments (1000); therefore, lower solubility (than in Fig. 3) could be expected in the actual system. However, the solubility experiments were used to assess the trend in relative solubilities of solid sodium silicates. The effect of sodium silicate silica modulus for BFS solubility in dry-mix mortars could be a topic for future studies. It is noticeable, that even though the solubility of Rm3.4 + NaOH reached almost 100%, similarly to Rm0.9, the Rm3.4 + NaOH does not reach high strength. This indicates that significant amount of NaOH is consumed for other reactions as well in actual mortar system. To adjust the silica modulus from 3.4 to 0.9, a higher dose of NaOH is required than can could be calculated based just on the SiO_2/Na_2O ratio of the activator.

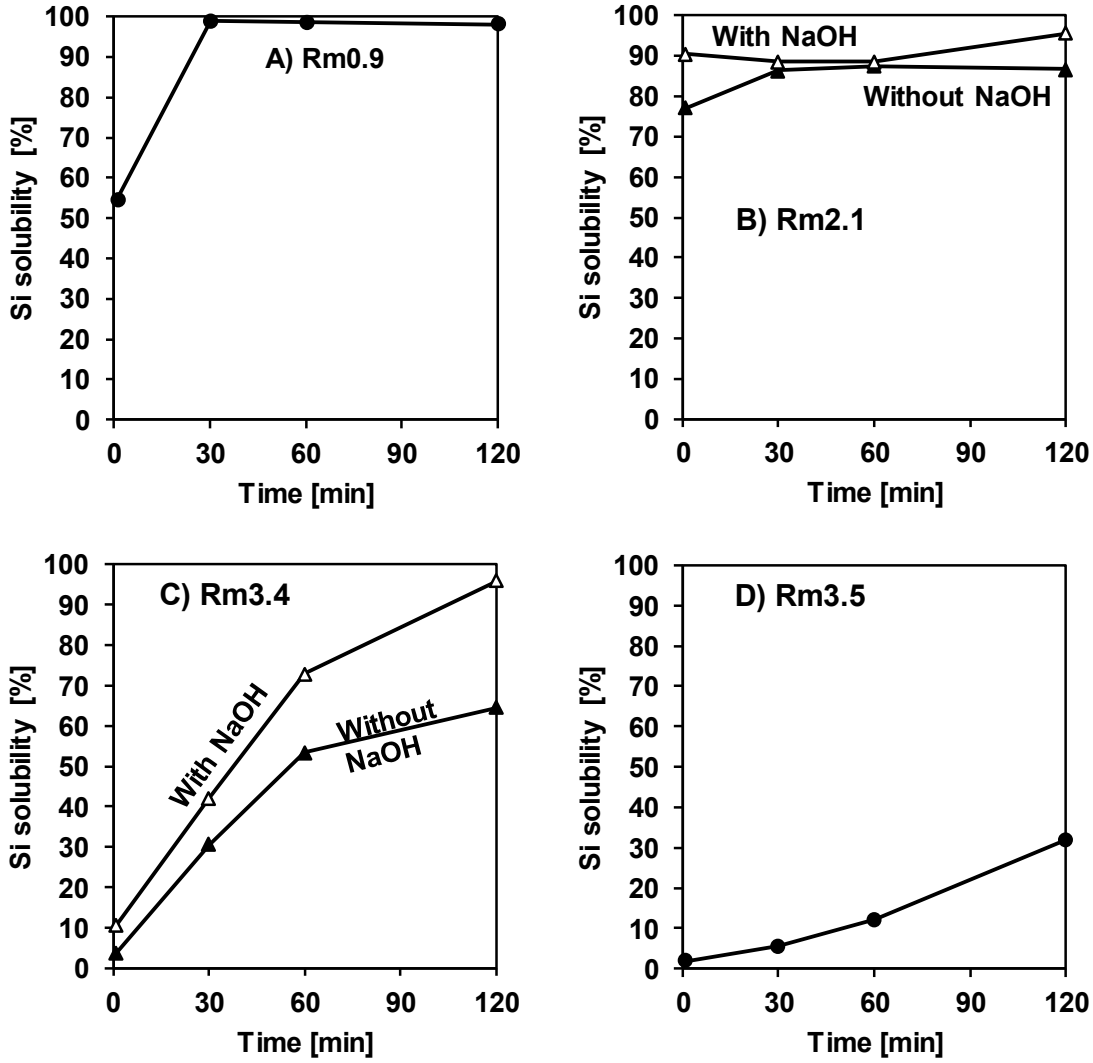

Fig. 3. Dissolution of sodium silicates (as a percentage of total Si) to deionized water (solid/liquid weight ratio = 0.001) as a function of time.

3.3 Isothermal calorimetry

The heat evolution curves of alkali-activated BFS can be classified in three groups: 1) only one peak; 2) initial peak, induction period, and accelerated hydration; and 3) two initial peaks, induction period, and accelerated hydration [41]. In the present study, the behavior followed group 1 or 2 (Fig. 4). The first peak (also referred to as pre-induction period) corresponds to the wetting and dissolution of the precursors and the second peak (also known as acceleration/deceleration) to the nucleation, growth and precipitation/condensation of the (C,N)-A-S-H gel [42-45]. Between the peaks, a dormant period can occur during which the soluble alumina and silica increase up to a specific threshold concentration required for gel formation [46].

The isothermal calorimetry results as normalized heat flow and cumulative heat flow are shown in Fig. 4 and Fig. 5, respectively. The mortars with Rm0.9, Rm2.1, Rm3.4, Rm3.4 + NaOH, and Rm3.5 exhibit two peaks of which the first appears at 3–5 min. This peak is likely a combination of dissolution of solid activator and precursor. Rm2.1 + NaOH exhibits only one peak, which could be because the two peaks have merged together. Therefore when NaOH is added to Rm2.1, it appears that dissolution and subsequent polymerization-condensation occur rapidly and simultaneously.

The intensity of the first peak (up to 73 mW/g with Rm0.9) is much lower compared to some studies in which BFS has been activated by solutions of NaOH and/or sodium silicate at 25 °C [47,48]. On the other hand, Zuo et al. [49] reported a slightly lower intensity of the first peak than in the present study when BFS was activated NaOH solution [49]. When NaOH is added (Rm2.1 + NaOH and Rm3.4 + NaOH) the initial heat release increases but stays lower than with Rm0.9. Nevertheless, these results indicate that the temperature increase in one-part dry mixtures of BFS and solid sodium silicate should be relatively moderate. This is supported also by existing studies as mortar activated by Rm0.9 (mass of mortar sample was 280 g) caused increase of approximately 10°C in semiadiabatic calorimetry in an earlier study by authors [18]. In a study by Collins and Sanjayan [50], concrete column with dimensions of 800 × 800 × 1200 mm^3 was prepared using BFS, sodium silicate powder, and hydrated lime as the binder. The maximum temperature difference in the center of the column to the surface was 10.5°C, which was approximately half of a similar column prepared of Portland cement-based concrete [50].

There is a clear difference in the appearance of the second peak between mortars prepared of different silicates. The timescale of the appearance of the second peak follows the order: Rm0.9 (≈ 700 min) > Rm2.1 (≈ 200 min) > Rm3.4 + NaOH (≈ 200 min) > Rm3.4 (≈ 50 min) > Rm3.5 (≈ 30 min). Interestingly, when NaOH is added to Rm2.1, the second peak disappears but with Rm3.4, the addition of NaOH delays the appearance of the second peak. Thus, it appears that the prolonged appearance of the second peak is beneficial for strength development (see Fig. 7). When these results are compared to the setting times (see Fig. 6), there is no clear correlation: initial and final setting can occur during the first peak, induction period, or second peak (see Fig. 6). However, interestingly, the heat maximum of the second peak is not greatly different between mortars prepared of different silicate grades and it follows the following trend: Rm0.9 (≈ 1.9 mW/g) ≈ Rm3.5 + NaOH (≈ 1.1 mW/g) > Rm3.4 (≈ 1.3 mW/g) > Rm2.1 (≈ 0.5 mW/g).

Heat release could cause shrinkage in the studied system and thus the shrinkage of the mortar activated with Rm0.9 (i.e., the highest heat release and presumably the highest shrinkage) was inspected (data shown in supplementary material). It was noticed that no shrinkage occurred when the specimen was kept at relative humidity of approximately 100%. At relative humidities of 60 and 23%, shrinkage stabilized at 30 d as approximately 3 and 4 mm/m, respectively.

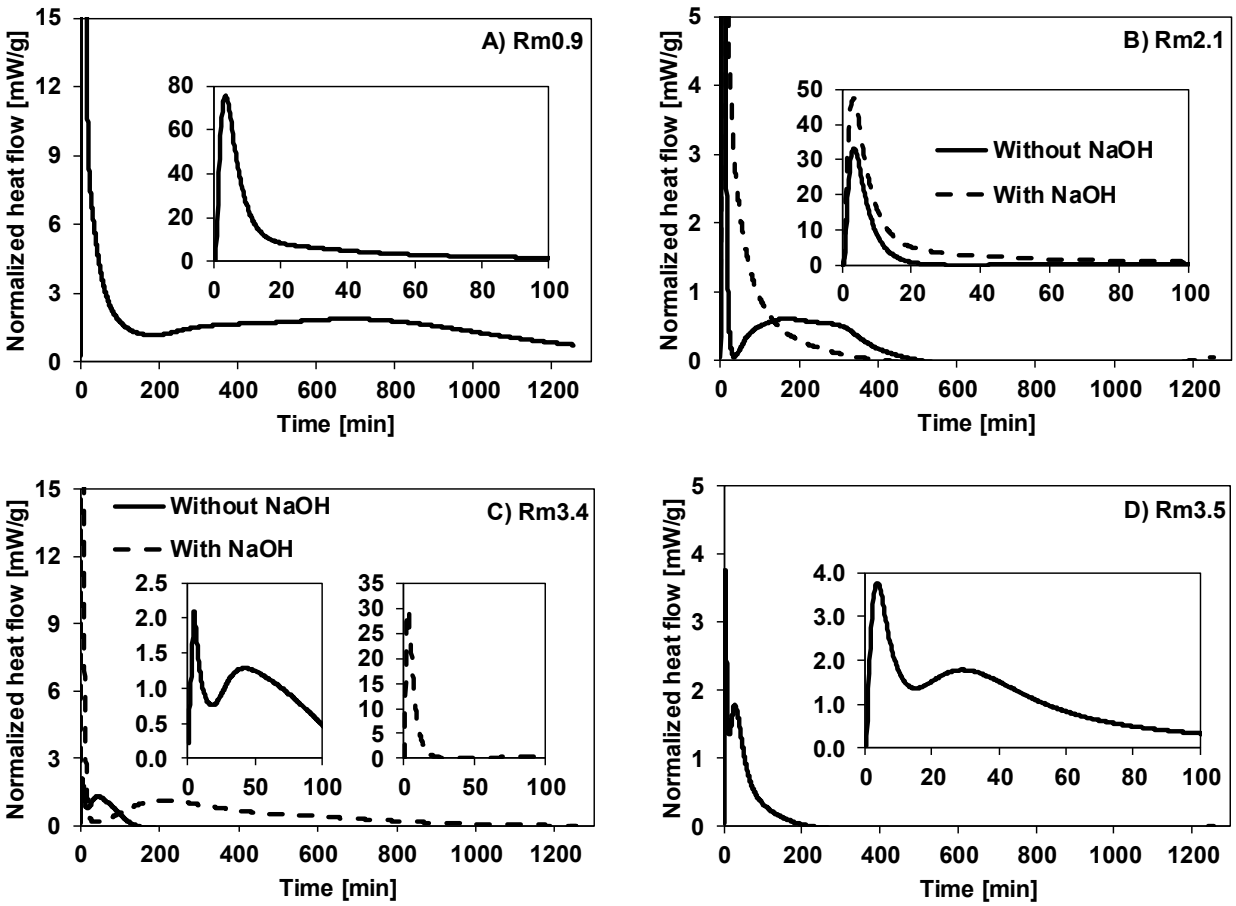

Fig. 4. Isothermal calorimetry curves of the mortars prepared using different sodium silicates. Results have been normalized by the mass of binder (i.e., BFS and solid sodium silicate).

The cumulative heat curves (Fig. 5) reveal also clear differences between samples. Rm0.9 produces the largest amount of heat (5–50-times that of the other silicates), the slope of heat cumulation changes at approximately 1 h. Rm0.9 continues to release heat for at least 20 h, while the other silicates reach their maximum much earlier. Rm2.1 exhibits a maximum in the cumulative heat at 8–9 h and after that, the value decreases. This indicates that some endothermic reactions take place, which could be related to the slow dissolution of solid sodium silicates (an endothermic reaction [51]). This observed decrease in the cumulated heat was confirmed to occur also in a repeated measurement. In the case of Rm2.1 + NaOH, the cumulative heat increases more rapidly and to a higher value than without NaOH. With Rm3.4, there is again a maximum and decrease in the cumulated heat, while with Rm3.4 + NaOH, there is a steep increase in the cumulative heat, which is followed by a plateau until 2 h. Then, the cumulative heat increases slowly (between approximately 2–12 h) to its maximum.

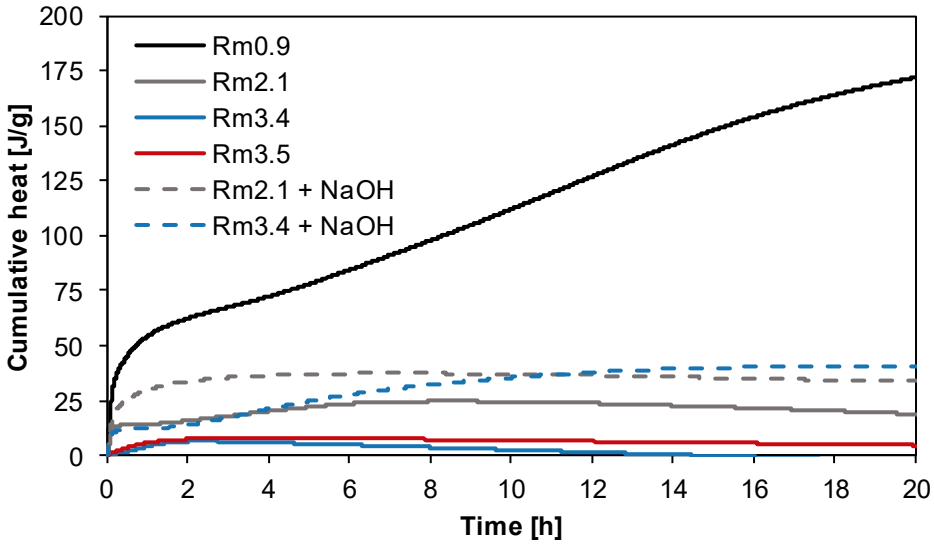

Fig. 5. Cumulative heat of the mortars prepared with different sodium silicates. Results have been normalized using binder (BFS, sodium silicate, and NaOH) mass.

3.4 Effect of silica modulus of sodium silicate on the fresh and hardened properties

The initial and final setting times increased as the silica modulus of the solid sodium silicate increased (Fig. 6). This is likely due to the faster reaction kinetics of the depolymerized silica species, which are present in silicates with a low silica modulus. Indeed, a negative correlation between final setting time and the amount of Q^1 and Q^2 exists, whereas with Q^3 and Q^4 the correlation is positive (see supplementary materials). Furthermore, the trend of Si dissolution rate (see Fig. 3) reflects the setting time results as it indicates how quickly saturation is reached. The addition of NaOH causes the setting time to increase in the case of Rm2.1 and to remain almost unchanged with Rm3.4. Possible explanation for this is that Rm2.1 already contains depolymerized silica; thus, the added NaOH reacts with the aluminosilicate network (i.e., the (C,N)-A-S-H gel) that is forming. Similar kind of phenomenon (i.e., partial depolymerization of aluminosilicate species during induction period) has been proposed to occur in the zeolite synthesis before the actual zeolite precipitation [52]. This depolymerization slows down the setting. In the case of Rm3.4, NaOH might be consumed for the depolymerization of the sodium silicate; therefore, it has little effect on final setting time. For construction purposes, the initial setting time should be at least 45 min [53]; only Rm3.5 + NaOH and Rm2.1 + NaOH can fulfil this requirement. However, in a previous work by the authors [18] it was found that that the setting time can be increased by decreasing the amount of solid sodium silicate while still ensuring sufficiently high compressive strength. Another alternative is to use retarding agents, such as nano-sized ZnO [54], sodium phosphate [55], phosphoric acid [56], lignosulfonate [57], or citric acid [58]. However, their suitability for one-part alkali-activated systems has not been documented. As a comparison to two-part alkali-activated BFS systems, Suraneni et al. [59] reported approximately similar initial and final setting times (30 and 40 min, respectively) as in the present study when using sodium hydroxide and silicate solutions as activators and penetration resistance as the test methods. As another example, Fernández-Jiménez and Puertas [37] obtained 90–165 and 100–230 min initial and final setting times using again mixtures of NaOH and sodium silicate. In general, one-part mixtures tend to send faster than two-part mixtures [2].

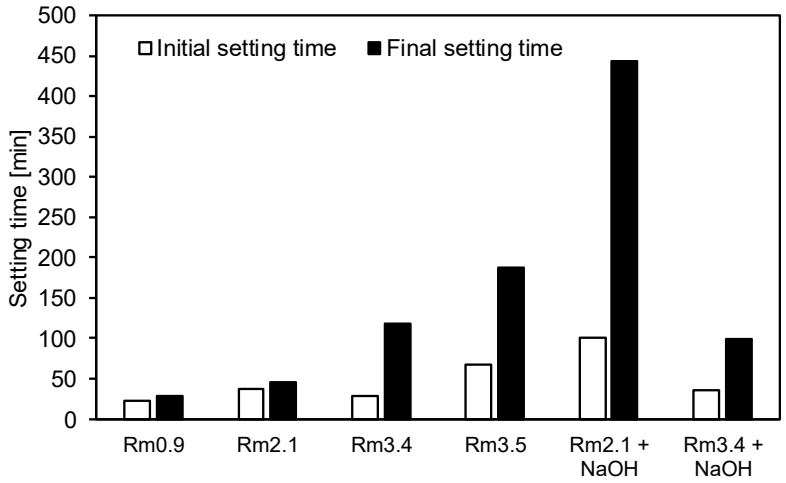

Fig. 6. Initial and final setting times of the mortars prepared with different sodium silicates.

The low silica modulus of the solid sodium silicate activator is associated with the high compressive strength development of mortar (Fig. 7). However, as the silica modulus increases from 2.1 to 3.4, there is a drastic decrease in the resulting strength. The same trend is also seen in two-part alkali-activated systems, as it is well known that the low silica modulus of the activator solution (i.e., the presence of less-connected Si centers) is related to the development of higher strength [60]. The optimum alkali-activator silica modulus for two-part blast furnace slag mortars systems has been reported to be 0.75–1.5 [4,61,62], which is in agreement with the results obtained with solid activators in the present study. However, it has been reported that using solid sodium silicate activator in comparison to a solution would result lower compressive strength [4]. Nevertheless, a systematic comparison of different solid and solution-form sodium silicate activators at different silica moduli is lacking and could represent an important subject for future studies. As mentioned in the section 2.2, the mortars prepared of Rm2.1, Rm3.4, and Rm3.5 contain 3.8, 4.7, and 3.9% more water than the mortar prepared of Rm0.9 due to the chemically bound water in sodium silicates. However, this extra water is not able to explain the large difference observed in compressive strength or in setting time.

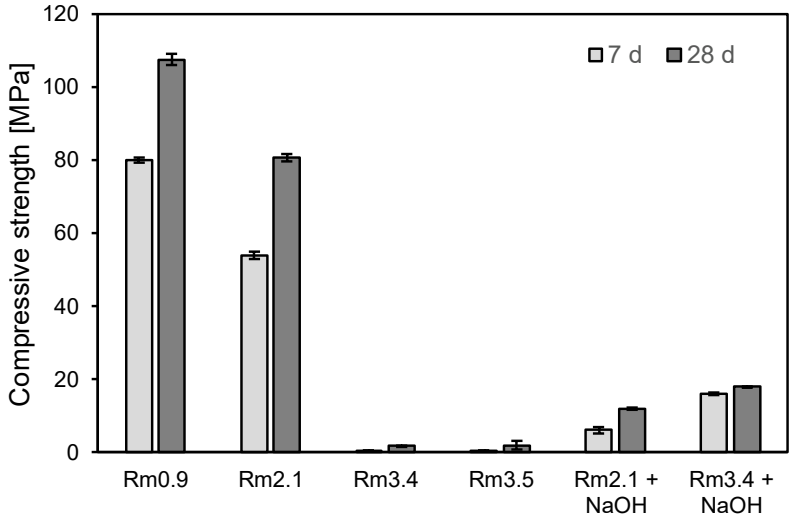

Fig. 7. Compressive strength (7 d and 28 d) resulting from sodium silicates with different silica moduli and sodium silicates with an NaOH-adjusted silica modulus.

In the case of Rm2.1, the addition of solid NaOH resulted in lower strength than with the unmodified activator; in contrast, in the case of Rm3.4, it resulted in higher strength. A similar observation has been made earlier in the literature when solid NaOH was mixed with sodium silicate powder with a low silica modulus (SiO_2/Na_2O = 0.9): increasing sodium hydroxide amount decreased compressive strength [63]. A possible explanation for this outcome is that sodium silicate with a low silica modulus, such as Rm2.1, is initially more depolymerized; therefore, added NaOH is consumed on depolymerizing the formed (C,N)-A-S-H gel [52]. However, with Rm3.4, the added NaOH is beneficial because it is consumed for depolymerizing the sodium silicate (which has a large amount of Q^3 and Q^4 Si environments) , thus providing more silicate species to the aqueous phase that can form (C,N)-A-S-H gel. This explanation is supported also by the setting time results (Fig. 6). Thus is can be hypothesized that when water is added to the mixture of the solid sodium silicate and blast furnace slag, NaOH can react in three possible ways: 1) it can depolymerize sodium silicate, 2) it can depolymerize the aluminosilicate precursor (BFS in this case), or 3) it can depolymerize the already formed aluminosilicate gel.

NaOH was mixed with Rm2.1 and Rm3.4 to modify the silica modulus so that it would be similar to that of Rm0.9. However, the results demonstrate that this modification does not lead to similar results between the modified silicates and Rm0.9. Ravikumar and Neithalath [17] used a solid activator with silica moduli of 0.62–1.55 for BFS by mixing NaOH and Na silicate. We showed in the present study that this kind of mixture is not comparable to solid sodium silicate with a similar modulus: for example Rm0.9 and Rm3.4 + NaOH in the present study both have a silica modulus of 0.9 but they result completely different fresh and hardened state properties in mortar. Based on these results, sodium silicate depolymerization appears to be the preferred reaction over depolymerization of the BFS or C-(N)-A-S-H gel. In contrast, in alkali-silicate solutions, it is possible to modify the silica modulus by adding alkali hydroxide [60], and this is a common practice. However, Essaidi et al. [64] compared alkali activators (all had R_M = 0.7) prepared by two methods: either adding NaOH pellets to a sodium silicate solution or mixing solid sodium silicate with water and adding NaOH pellets. They noticed that the activator solution prepared with solid silicate contained more polymerized silica than the one prepared with the silicate solution [64]. These findings further emphasize the different behavior of one and two-part systems.

3.5 Phase composition

Diffractograms of pastes at 28 d age are shown in Fig. 8. The Rietveld analysis (with 10 wt% of rutile as internal standard) revealed that the pastes were over 99 wt% amorphous with the exception of Rm0.9, which contained approximately 2 wt% hydrotalcite. Hydrotalcite-like phases (general formula $M_x^{2+}M_y^{3+}(OH)_{2x+3y-nz}(A^{n-})_z \cdot mH_2O$, where M_x^{2+}, M_y^{3+}, and A^{n-} are commonly Mg^{2+}, Al^{3+}, and CO_3^{2-}, respectively, in the BFS systems and x/y between 2–3 [65-67]) are formed when the MgO content of the precursor BFS is higher than 5 wt% [68]. The hydrotalcite-like phases have a Mg/Al molar ratio between 2–3 [67], which is typically observed after a prolonged curing (in one study after 90 d [69]). The availability of Mg and Al are in part controlled by the pH, which is the highest with sodium silicate Rm0.9 (see Fig. 2). Thus this could explain the formation of hydrotalcite in this sample. However, the hydrotalcites formed with sodium silicate activators have been reported to be of low structural ordering [66,70,71], which could be also the case in the present study. The peak in the amorphous halo (between approximately 30–40 °2θ) indicates that the amount of the weakly ordered (C,N)-A-S-H gel decreases (i.e., peak intensity decreases) as the silica modulus increases. However, when sodium hydroxide is added, there is a clearly visible peak although the mechanical strength of the mortars was low. It appears that the peak in the amorphous halo follows the trend observed with pH: the strongest peak is observed with Rm0.9, Rm2.1 + NaOH, and Rm3.4 + NaOH, which had the highest pH. Zuo et al. [72] studied the pore solutions of blast furnace slag activated with different alkali activators. They observed that amount of OH^- decreased as a function of time and the concentration of Al

and Si in pore solution increased as the concentration of OH^- increased [72]. Therefore, the estimated initial pH of mortars (see section 3.2) reflect the availability of Si and Al required for oversaturation and subsequent (C,N)-A-S-H formation. Moreover, Zuo et al. [72] also reported that NaOH as an alkali activator induced more ordered calcium aluminosilicate hydrate structure leading to a stronger (C,N)-A-S-H peak. A larger dose of NaOH (i.e., higher pH) increased the (C,N)-A-S-H peak intensity as well [72], which is in agreement with the present finding.

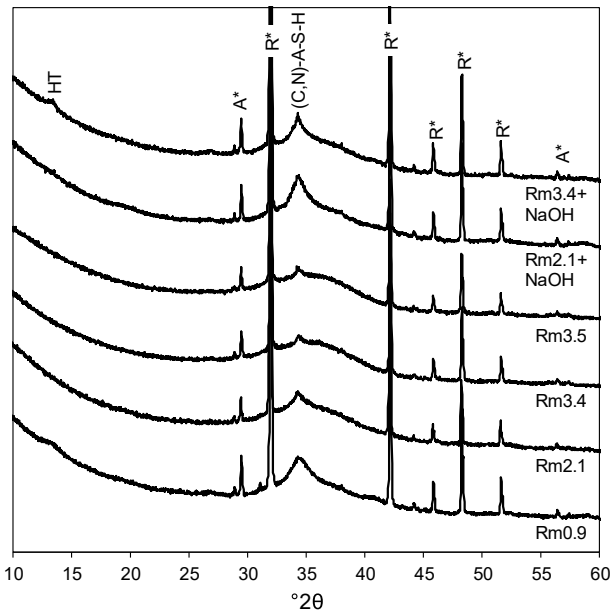

Fig. 8. Diffractograms of pastes prepared with different sodium silicates at 28 d age. HT = hydrotalcite ($Mg_6Al_2CO_3(OH)_{16}{\cdot}4H_2O$), R* = rutile, internal standard (TiO_2), A* = anatase, internal standard (TiO_2).

4. Conclusions

The type of solid sodium silicate affects significantly for the fresh and hardened properties of one-part alkali-activated blast furnace slag mortar. The present study focused on the silica modulus (SiO_2/Na_2O ratio) as one of the most important properties when selecting the solid sodium silicate activator. The following main conclusions can be made based on the results:

1. A low silica modulus of solid sodium silicate indicates the presence of less polymerized silica, higher pH, and faster dissolution. The results indicate that the Q^1 and Q^2 are the essential Si environments in solid sodium silicate resulting high strength development since they are less polymerized and readily available for reactions.
2. When the silica modulus of solid sodium silicate decreases, the strength of the obtained one-part alkali-activated slag increases at both 7 and 28 d, which is in agreement with earlier literature. Together with that trend, setting time decreases and the heat released during setting and hardening increases. The amount of weakly ordered (C,N)-A-S-H gel is higher and traces of hydrotalcite-like phases are present when using a low silica modulus activator. A boundary silica modulus that defines whether the solid sodium silicate can be used in practice as a one-part alkali-activated slag mortar activator was found between 2.1 and 3.4 (the lower, the better).

3. When solid NaOH is mixed with solid sodium silicate to adjust the silica modulus (i.e., decrease it by adding Na_2O), the obtained outcome in terms of mortar properties depend on the silica modulus of the sodium silicate. NaOH together with a low silica modulus sodium silicate results decreased fresh and hardened state properties compared to a situation without NaOH. It was hypothesized that NaOH is partially consumed for degrading the formed (C,N)-(A)-S-H gel. However, NaOH together with a high silica modulus sodium silicates improves the fresh and hardened state properties in contrast to a situation without NaOH. This is a result of NaOH depolymerizing sodium silicate Q^3 and Q^4 silicon environments.

Finally, it should be also noted that the standard mortar mix design (according to EN 196) might not result optimum fresh and hardened state properties when preparing one-part alkali-activated slag mortars. In the present study, a lower water content than suggested by the standard was found to be the optimum.

Acknowledgements

This work was supported by the Finnish Funding Agency for Technology and Innovation (Tekes) (project GEOBIZ, grant number 1105/31/2016). Anu Kantola and Ville-Veikko Telkki acknowledge the financial support received from the Kvantum Institute (University of Oulu) and the Academy of Finland (grants #289649 and 294027). The authors wish to thank Viljami Viinikka for contributing to the preparation of the specimens.

References

[1] J.L. Provis, Alkali-activated materials, Cem. Concr. Res. 114 (2018) 40-48.

[2] T. Luukkonen, Z. Abdollahnejad, J. Yliniemi, P. Kinnunen, M. Illikainen, One-part alkali-activated materials: A review, Cem. Concr. Res. 103 (2018) 21-34.

[3] A. Purdon, The action of alkalis on blast-furnace slag, J. Soc. Chem. Ind. 59 (1940) 191-202.

[4] S. Wang, K.L. Scrivener, P.L. Pratt, Factors affecting the strength of alkali-activated slag, Cem. Concr. Res. 24 (1994) 1033-1043.

[5] K. Neupane, Fly ash and GGBFS based powder-activated geopolymer binders: A viable sustainable alternative of portland cement in concrete industry, Mech. Mater. 103 (2016) 110-122.

[6] K. Neupane, D. Chalmers, P. Kidd, High-Strength Geopolymer Concrete- Properties, Advantages and Challenges, Adv. Mat. 7 (2018) 15-25.

[7] D.P. Chalmers, P.G. Kidd, P.D. Sleep, Geopolymer cement, US Patent US20150321954A1 (2015).

[8] A. Hajimohammadi, J.S.J. van Deventer, Solid Reactant-Based Geopolymers from Rice Hull Ash and Sodium Aluminate, Waste Biomass Valor. 8 (2016) 2131-2140.

[9] A. Peys, H. Rahier, Y. Pontikes, Potassium-rich biomass ashes as activators in metakaolin-based inorganic polymers, Appl. Clay. Sci. 119 (2016) 401-409.

[10] A. Peys, L. Arnout, B. Blanpain, H. Rahier, K. van Acker, Y. Pontikes, Mix-design Parameters and Real-life Considerations in the Pursuit of Lower Environmental Impact Inorganic Polymers, Waste Biomass Valor. (2017) 1-11.

[11] F. Puertas, M. Torres-Carrasco, Use of glass waste as an activator in the preparation of alkali-activated slag. Mechanical strength and paste characterisation, Cem. Concr. Res. 57 (2014) 95-104.

[12] J.L. Provis, Introduction and scope, in: J.L. Provis, J.S.J. Van Deventer (Eds.), Alkali Activated Materials, State-of-the-Art Report, RILEM TC 224-AAM, Springer, Dordrecht, 2014, pp. 1-9.

[13] A. Heath, K. Paine, M. McManus, Minimising the global warming potential of clay based geopolymers, J. Clean. Prod. 78 (2014) 75-83.

[14] C. Ma, G. Long, Y. Shi, Y. Xie, Preparation of cleaner one-part geopolymer by investigating different types of commercial sodium metasilicate in China, J. Clean. Prod. 201 (2018) 636-647.

[15] B. Nematollahi, J. Sanjayan, F.U.A. Shaikh, Synthesis of heat and ambient cured one-part geopolymer mixes with different grades of sodium silicate, Ceram. Int. 41 (2015) 5696-5704.

[16] F. Collins, J.G. Sanjayan, Early age strength and workability of slag pastes activated by sodium silicates, Mag. Concr. Res. 53 (2001) 321-326.

[17] D. Ravikumar, N. Neithalath, Effects of activator characteristics on the reaction product formation in slag binders activated using alkali silicate powder and NaOH, Cem. Concr. Compos. 34 (2012) 809-818.

[18] T. Luukkonen, Z. Abdollahnejad, J. Yliniemi, P. Kinnunen, M. Illikainen, Comparison of alkali and silica sources in one-part alkali-activated blast furnace slag mortar, J. Clean. Prod. 187 (2018) 171-179.

[19] K.H. Yang, J.K. Song, A.F. Ashour, E.T. Lee, Properties of cementless mortars activated by sodium silicate, Constr. Build. Mater. 22 (2008) 1981-1989.

[20] K.H. Yang, J.K. Song, K.S. Lee, A.F. Ashour, Flow and compressive strength of alkali-activated mortars, ACI Mater. J. 106 (2009) 50-58.

[21] K.H. Yang, J.K. Song, J.S. Lee, Properties of alkali-activated mortar and concrete using lightweight aggregates, Mater. Struct. 43 (2010) 403-416.

[22] F. Collins, J.G. Sanjayan, Microcracking and strength development of alkali activated slag concrete, Cem. Concr. Compos. 23 (2001) 345-352.

[23] F.G. Collins, J.G. Sanjayan, Workability and mechanical properties of alkali activated slag concrete, Cem. Concr. Res. 29 (1999) 455-458.

[24] F. Collins, J.G. Sanjayan, Strength and shrinkage properties of alkali-activated slag concrete containing porous coarse aggregate, Cem. Concr. Res. 29 (1999) 607-610.

[25] F. Collins, J.G. Sanjayan, Effects of ultra-fine materials on workability and strength of concrete containing alkali-activated slag as the binder, Cem. Concr. Res. 29 (1999) 459-462.

[26] M. Criado, A. Fernández-Jiménez, A. Palomo, I. Sobrados, J. Sanz, Effect of the SiO2/Na2O ratio on the alkali activation of fly ash. Part II: 29Si MAS-NMR Survey, Microporous Mesoporous Mater. 109 (2008) 525-534.

[27] L. Kobera, R. Slavík, D. Koloušek, M. Urbanová, J. Kotek, J. Brus, Structural stability of aluminosilicate inorganic polymers: Influence of the preparation procedure, Ceram Silikaty. 55 (2011) 343-354.

[28] J. Mahler, A. Sebald, Deconvolution of29Si magic-angle spinning nuclear magnetic resonance spectra of silicate glasses revisited - some critical comments, Solid State Nucl. Magn. Reson. 5 (1995) 63-78.

[29] J.B. Murdoch, J.F. Stebbins, High-resolution ^{29}Si NMR study of silicate and aluminosilicate glasses: the effect of network-modifying cations, Am. Min. 70 (1985) 332-343.

[30] Finnish Standard Association (SFS), Water quality. Determination of selected elements by inductively coupled plasma optical emission spectrometry (ICP-OES) (SFS-EN ISO 11885), Finnish Standard Association, Helsinki, 2009.

[31] European Committee for Standardization (CEN), Methods of Testing Cement. Part 3: Determination of Setting Times and Soundness (EN 196-3), European Committee for Standardization, Brussels, 2016.

[32] European Committee for Standardization (CEN), Methods of Testing Cement. Part 1: Determination of Strength (EN 196-1), European Committee for Standardization, Brussels, 2016.

[33] A. Gharzouni, E. Joussein, B. Samet, S. Baklouti, S. Pronier, I. Sobrados, J. Sanz, S. Rossignol, The effect of an activation solution with siliceous species on the chemical reactivity and mechanical properties of geopolymers, J. Sol Gel Sci. Technol. 73 (2014) 250-259.

[34] L. Vidal, E. Joussein, M. Colas, J. Cornette, J. Sanz, I. Sobrados, J.-. Gelet, J. Absi, S. Rossignol, Controlling the reactivity of silicate solutions: A FTIR, Raman and NMR study, Colloids Surf. A Physicochem. Eng. Asp. 503 (2016) 101-109.

[35] B. Walkley, J.L. Provis, Solid-state nuclear magnetic resonance spectroscopy of cements, Mat. Today Adv. 1 (2019) 100007.

[36] M.T. Tognonvi, D. Massiot, A. Lecomte, S. Rossignol, J. Bonnet, Identification of solvated species present in concentrated and dilute sodium silicate solutions by combined ^{29}Si NMR and SAXS studies, J. Coll. Interf. Sci. 352 (2010) 309-315.

[37] A. Fernández-Jiménez, F. Puertas, Effect of activator mix on the hydration and strength behaviour of alkali-activated slag cements, Adv. Cem. Res. 15 (2003) 129-136.

[38] G. Lagaly, W. Tufar, A. Minihan, A. Lovell, Silicates, in: Ullmann's Encyclopedia of Industrial Chemistry, Electronic Release, Wiley-VCH, Weinheim, 2000.

[39] J. Davidovits, Geopolymer Chemistry & Applications, 3rd ed., Institut Geopolymere, Saint-Quentin, 2011.

[40] R.K. Iler, The Chemistry of Silica. Solubility, Polymerization, Colloid and Surface Properties, and Biochemistry, John Wiley & Sons, New York, 1979.

[41] C. Shi, R.L. Day, A calorimetric study of early hydration of alkali-slag cements, Cem. Concr. Res. 25 (1995) 1333-1346.

[42] S. Puligilla, P. Mondal, Role of slag in microstructural development and hardening of fly ash-slag geopolymer, Cem. Concr. Res. 43 (2013) 70-80.

[43] S. Kumar, R. Kumar, S.P. Mehrotra, Influence of granulated blast furnace slag on the reaction, structure and properties of fly ash based geopolymer, J. Mater. Sci. 45 (2010) 607-615.

[44] S. Alonso, A. Palomo, Alkaline activation of metakaolin and calcium hydroxide mixtures: influence of temperature, activator concentration and solids ratio, Mater. Lett. 47 (2001) 55-62.

[45] M. Criado, B. Walkley, X. Ke, J.L. Provis, S.A. Bernal, Slag and activator chemistry control the reaction kinetics of sodium metasilicate-activated slag cements, Sustainability. 10 (2018).

[46] Z. Sun, A. Vollpracht, Isothermal calorimetry and in-situ XRD study of the NaOH activated fly ash, metakaolin and slag, Cem. Concr. Res. 103 (2018) 110-122.

[47] A.R. Brough, A. Atkinson, Sodium silicate-based, alkali-activated slag mortars - Part I. Strength, hydration and microstructure, Cem. Concr. Res. 32 (2002) 865-879.

[48] A. Fernández-Jiménez, F. Puertas, Alkali-activated slag cements: Kinetic studies, Cem. Concr. Res. 27 (1997) 359-368.

[49] Y. Zuo, M. Nedeljkovic, G. Ye, Coupled thermodynamic modelling and experimental study of sodium hydroxide activated slag, Constr. Build. Mater. 188 (2018) 262-279.

[50] F. Collins, J.G. Sanjayan, Strength and shrinkage properties of alkali-activated slag concrete placed into a large column, Cem. Concr. Res. 29 (1999) 659-666.

[51] C. Shi, D. Roy, P. Krivenko, Alkali-Activated Cements and Concretes, CRC Press, Boca Raton, 2006.

[52] L. Itani, Y. Liu, W. Zhang, K.N. Bozhilov, L. Delmotte, V. Valtchev, Investigation of the physicochemical changes preceding zeolite nucleation in a sodium-rich aluminosilicate gel, J. Am. Chem. Soc. 131 (2009) 10127-10139.

[53] European Committee for Standardization (CEN), Cement - Part 1: Composition, Specifications and Conformity Criteria for Common Cements (EN 197-1), European Committee for Standardization, Brussels, 2000.

[54] N. Garg, C.E. White, Mechanism of zinc oxide retardation in alkali-activated materials: an in situ X-ray pair distribution function investigation, J. Mat. Chem. A. 5 (2017) 11794-11804.

[55] C. Gong, N. Yang, Effect of phosphate on the hydration of alkali-activated red mud–slag cementitious material, Cem. Concr. Res. 30 (2000) 1013-1016.

[56] J.J. Chang, A study on the setting characteristics of sodium silicate-activated slag pastes, Cem. Concr. Res. 33 (2003) 1005-1011.

[57] T. Luukkonen, Z. Abdollahnejad, K. Ohenoja, P. Kinnunen, M. Illikainen, Suitability of commercial superplasticizers for one-part alkali-activated blast-furnace slag mortar, J. Sustain. Cem. Based Mater. 8 (2019) 244-257.

[58] L. Xu, F. Matalkah, P. Soroushian, N. Darsanasiri, S. Hamadneh, W. Wu, Effects of citric acid on the rheology, hydration and strength development of alkali aluminosilicate cement, Adv. Cem. Res. 30 (2017) 75-82.

[59] P. Suraneni, S. Puligilla, E.H. Kim, X. Chen, L.J. Struble, P. Mondal, Monitoring Setting of Geopolymers, Adv. Civ. Eng. Mat. 3 (2014) 1-17.

[60] A. Gharzouni, E. Joussein, B. Samet, S. Baklouti, S. Rossignol, Effect of the reactivity of alkaline solution and metakaolin on geopolymer formation, J. Non Cryst. Solids. 410 (2015) 127-134.

[61] D. Krizan, B. Zivanovic, Effects of dosage and modulus of water glass on early hydration of alkali-slag cements, Cem. Concr. Res. 32 (2002) 1181-1188.

[62] T. Bakharev, J.G. Sanjayan, Y.-. Cheng, Alkali activation of Australian slag cements, Cem. Concr. Res. 29 (1999) 113-120.

[63] K.H. Yang, J.K. Song, Workability loss and compressive strength development of cementless mortars activated by combination of sodium silicate and sodium hydroxide, J. Mater. Civ. Eng. 21 (2009) 119-127.

[64] N. Essaidi, L. Laou, S. Yotte, L. Ulmet, S. Rossignol, Comparative study of the various methods of preparation of silicate solution and its effect on the geopolymerization reaction, Results Phys. 6 (2016) 280-287.

[65] S. Miyata, Physico-chemical properties of synthetic hydrotalcites in relation to composition, Clay Miner. 23 (1975) 369.

[66] X. Ke, S.A. Bernal, J.L. Provis, Controlling the reaction kinetics of sodium carbonate-activated slag cements using calcined layered double hydroxides, Cem. Concr. Res. 81 (2016) 24-37.

[67] S.J. Mills, A.G. Christy, J.-.R. Génin, T. Kameda, F. Colombo, Nomenclature of the hydrotalcite supergroup: Natural layered double hydroxides, Mineral. Mag. 76 (2012) 1289-1336.

[68] J.L. Provis, S.A. Bernal, Geopolymers and related alkali-activated materials, Annu. Rev. Mater. Res. 44 (2014) 299-327.

[69] J.I. Escalante-García, A.F. Fuentes, A. Gorokhovsky, P.E. Fraire-Luna, G. Mendoza-Suarez, Hydration products and reactivity of blast-furnace slag activated by various alkalis, J. Am. Ceram. Soc. 86 (2003) 2148-2153.

[70] F. Puertas, A. Fernández-Jiménez, M.T. Blanco-Varela, Pore solution in alkali-activated slag cement pastes. Relation to the composition and structure of calcium silicate hydrate, Cem. Concr. Res. 34 (2004) 139-148.

[71] M. Ben Haha, G. Le Saout, F. Winnefeld, B. Lothenbach, Influence of activator type on hydration kinetics, hydrate assemblage and microstructural development of alkali activated blast-furnace slags, Cem. Concr. Res. 41 (2011) 301-310.

[72] Y. Zuo, M. Nedeljkovic, G. Ye, Pore solution composition of alkali-activated slag/fly ash pastes, Cem. Concr. Res. 115 (2019) 230-250.